Journal of Sciences, Islamic Republic of Iran 31(1): 39 - 43 (2020) http://jsciences.ut.ac.ir
University of Tehran, ISSN 1016-1104

Synthesis of Fe-doped CeO_2 Nanoparticles Prepared by Solgel Method

M. Farahmandjou* and M. Dastpak

Department of Physics, Varamin Pishva Branch, Islamis Azad University, Varamin, Islamic Republic of Iran

Received: 2 June 2018 / Revised: 1 June 2019 / Accepted: 21 December 2019

Abstract

Nanomaterials have achieved remarkable technological advances in bulk materials due to their excellent physical, chemical and biological properties. cerium oxide (CeO_2) nanostructured doped with Fe ions is attractive due to improvement in redox properties, transport property and surface-to-volume ratio. In this research, Fe-doped CeO_2 nanoparticles (NPs) were prepared by simple solgel method. The as-synthesized and annealed samples were studied by transmission electron microscopy (TEM), field emission scanning electron microscopy (FESEM) and x-ray diffraction (XRD). The XRD result revealed the cubic crystal structure of Fe-doped CeO_2 NPs. The FESEM images showed that the uniformity of the NPs increase with increasing calcination temperature. The TEM studies demonstrated the 20 nm uniform NPs.

Keywords: Fe/CeO_2 nanoparticles; Crystal structure; Solgel; Chemical synthesis.

Introduction

Metal oxide semiconductor (MOS) NPs have greatly applications such as magnetic recording media, nanocatalysis and biology sciences [1–28]. Nanostructured materials are one of the most popular materials in science and engineering and will have many applications in the coming technologies [29-36].

Due to excellent physical and chemical properties such as fuel cells, CeO_2 has recently received much attention [37]. Cerium oxide is one of the most important rare earth metal oxides and has many applications in the industry, including in solid oxide catalysts and fuel cells. Cerium oxide, as a relatively high dielectric constant, has attracted researchers' attention in applications such as dielectric capacitors available in dynamically accessible memory and oxygen sensors. Another important application is magnetic oxides diluted at a temperature higher than room temperature, creating a new classification for the study of magnetic properties. This kind of oxide has a potential electrolyte for medium-temperature solid oxide fuel cells and has recently become a promising material for second-generation spintronics due to the ferromagnetic properties observed at room temperature. Nanostructured materials based on CeO_2 have achieved significant impact in practical applications due to the overall improvement of catalytic, electrical and optical properties. Solid oxide fuel cell technology is currently the most suitable field in which CeO_2 applications can be found. CeO_2 is a semiconductor with UV ($\lambda \geq$ 388nm, E_g= 3.2eV) and visible light absorption.

Defects of CeO_2 include rapid formation and

* Corresponding author: Tel: +982122495632; Fax: +982122340298; Email: farahmandjou@iauvaramin.ac.ir

elimination, and formation in the concentrated or decentralized 4f electron layer. The doping element needs to be biocompatible. In that context, Fe^{3+} seems to be a good candidate for cosmetic application, which has not yet been studied for UV filtration applications. Indeed, this biocompatible element has a lower valence state than Ce^{4+}, as well as being cheap and abundant. Furthermore, it can bring a brown color to the CeO_2 phase, which is naturally pale yellow in colour,and thus give a brown tinge to the final product [38]. High oxygen storage capacity is one kind of applications of Fe-doped CeO_2.

Fe^{3+}-doped CeO_2 nanocrystals have been prepared by various methods such as sol–gel [39], hydrothermal [40], coprecipitation method [41] and ball milling process [42]. Among these methods, the sol gel method has been widely used for easy reaction control and synthesis of single-size nanoparticles [17].

Materials and Methods

Fe-doped CeO_2 NPs were fabricated by a simple solgel synthesis. Firstly, 3g $CeCl_2 \cdot 5H_2O$ was dissolved in 100 mL pure water and then 3g $FeCl_3.6H_2O$ was disolved to the solution and then stirred at room temperature for 10 min and finally synthesis temperature was increased to 85°C. The pH=4 was adjusted during the fabrication. The product were synthesized for 3 hours and annealed at 500°C for 3 hours. The crystal structure and morphology of the as-prepared and calcined NPs were done by XRD, FESEM and TEM analyses.

Results and Discussion

Crystal structure and crystalline phases was identified by XRD analysis. Figure 1 shows the XRD spectra of the sample after calcination at 500 °C for 3 hours. The peaks, which were formed at 2θ angles of 28.67°, 33.25°, 47.59°, 56.45°, 69.53°, 76.80° and 79.16°, were indexed to the x-ray reflections of (111), (200), (220), (311), (400), (331) and (420) respectively, representing the cubic structure (according JCPDS Card no. 21-1272). The average size of the NPs has been determined by Sherrer formula [43].

The crystallite size for as-synthesized sample was determined in the range size of 15-25 nm from the Sherrer formula. The results showed that iron impurities ions penetrate the crystalline network of cerium oxide nanoparticles and decrease their size in the boundaries. In addition, the increase in iron ions dopant increases the depletion in the Ce network through the oxygen present in the crystalline network, thereby reducing the size of the nanoparticles. In fact, doped ions of iron are dispersed in the CeO_2 lattice and replaced with cerium atoms. In addition, decrease in the size of the particles is due to adding Fe atoms on the surface of the nanoparticles.

In order to specify the morphology of the samples, FESEM analysis was used for as-prepared and annealed

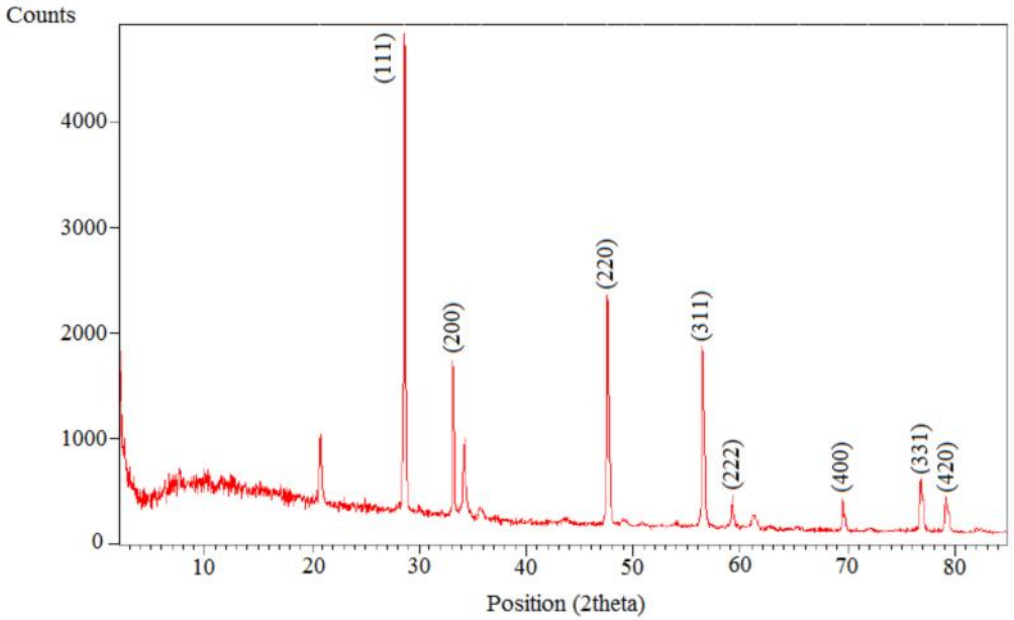

Figure 1. XRD pattern of annealed Fe-doped CeO_2 sample

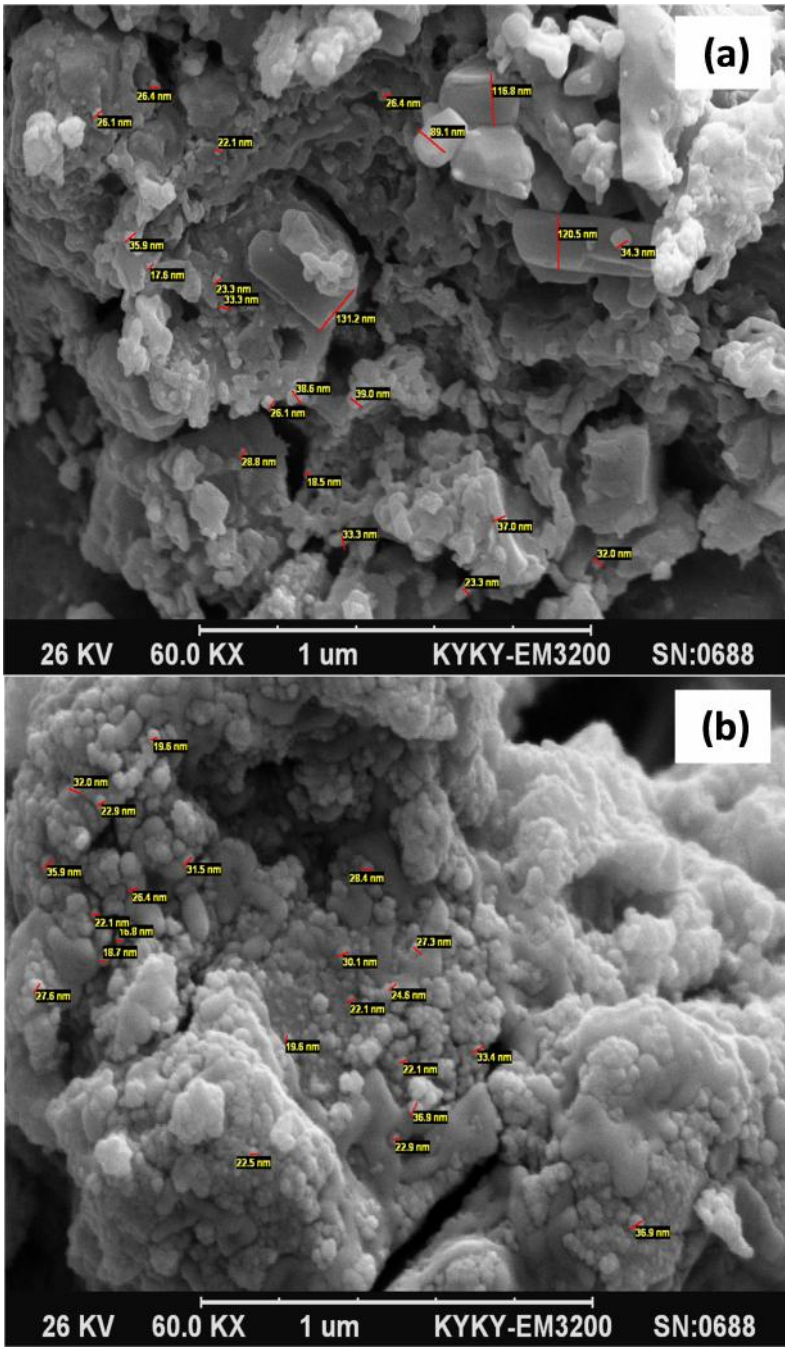

Figure 2. FESEM images of the (a) as-prepared (b) annealed Fe-doped CeO_2 NPs at 500 ^oC

NPs. Figure 2(a) reveals the FESEM image of the as-synthesized Fe-doped CeO_2 NPs. Figure 2(b) demonstrates the FESEM image of the heated FeCe NPs at 500^oC for 3 hours. The FESEM analysis shows that the uniformity of the particles increase with increasing annealing temperature. In fact, the interatomic forces increase with decreasing size of the nanoparticles, causing the nanoparticles to become closer to each other, resulting in their aggregation. The results is in correspondence with the average size of the nanoparticles measured by XRD analysis.

To estimate the actual size and shape of the NPs

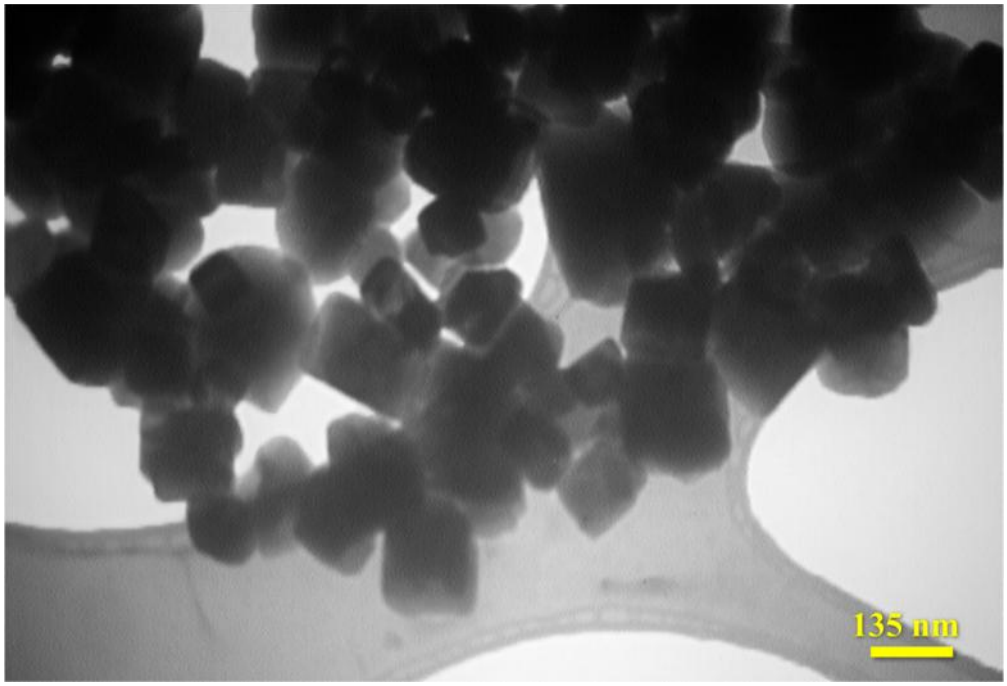

Figure 3. TEM image of the as-synthesized Fe-doped CeO_2 NPs

TEM analysis was carried out. Figure 3 shows the as-prepared TEM image of Fe/CeO_2 NPs with mean diameter of 20 nm prepared by solgel method. TEM also shows that the particles have been aggregated, which is due to the removal carboxylic group at 500°C.

Conclusions

Fe/CeO_2 NPs have been fabricated using simple solgel method. XRD spectrum shows single-crystal with face-centered cubic crystal cell of the CeO_2 structure and crystallizes in the cubic Fm-3m space group. FESEM images showed that the uniformity of the annealed NPs increased with less agglomeration. TEM image exhibits good uniformity of the as-prepared Fe-doped CeO_2 NPs with a mean diameter of 20 nm.

References

1. Zarinkamar M., Farahmandjou M. and Firoozabadi T.P. Diethylene Glycol-Mediated Synthesis of Nano-Sized Ceria (CeO_2) Catalyst. *J. Nanostruct.* **6**: 116-120 (2016).
2. Farahmandjou M. and Khalili P. Morphology Study of anatase nano-TiO_2 for Self-cleaning Coating. *Int. J. Fund. Phys. Sci.* **3**: 54-56 (2013).
3. Ramazani M., Farahmandjou M. and Firoozabadi. T.P. Fabrication and Characterization of Rutile TiO_2 Nanocrystals by Water Soluble Precursor. *Phys. Chem. Res.* **3**: 293-298 (2015).
4. Khoshnevisan B., Marami M.B. and Farahmandjou M. Fe^{3+}-Doped Anatase TiO_2 Study Prepared by New Sol-Gel Precursors. *Chin. Phys. Lett.* **35**: 027501-5 (2018).
5. Marami M.B., Farahmandjou M. and Khoshnevisan B. Solgel Synthesis of Fe-doped TiO_2 Nanocrystals. *J. electron. Mater.* **47**: 3741-3748 (2018).
6. Jafari, A., Khademi S. and Farahmandjou M. Nano-crystalline Ce-doped TiO_2 Powders: Sol-gel Synthesis and Optoelectronic Properties. *Mater. Res. Express.* 2018, **5**: 095008 (2018).
7. Farahmandjou M. and Khalili P. Study of Nano SiO_2/TiO_2 Superhydrophobic Self-Cleaning Surface Produced by Sol-Gel. *Aust. J. Basic. Appl. Sci.* 2013, **7**: 462-465 (2013).
8. Jurablu. S., Farahmandjou M. and Firoozabadi T.P. Sol-gel synthesis of zinc oxide (ZnO) nanoparticles: study of structural and optical properties. *J. Sci. I. R. Iran.* **26**: 281-285 (2015).
9. Farahmandjou M. and Dastpak M. Fe-Loaded CeO_2 Nanosized Prepared by Simple Co-Precipitation Route. *Phys. Chem. Res.* **6**: 713-720 (2018).
10. Farahamndjou M. The study of electro-optical properties of nanocomposite ITO thin films prepared by e-beam evaporation. *Rev. Mex. Fís.* **59**: 205-207 (2013).
11. Akhtari F., Zorriasatein S., Farahmandjou M. and Elahi S.M. Structural, optical, thermoelectrical, and magnetic study of $Zn_{1-x}Co_xO$ ($0 \leq x \leq 0.10$) nanocrystals. *Int. J. Appl. Ceram. Technol.* **15**: 723-733 (2018).
12. Akhtari F., Zorriasatein S., Farahmandjou M. and Elahi S.M. Synthesis and optical properties of Co^{2+}-doped ZnO Network prepared by new precursors. *Mater. Res. Express.* **5**: 065015 (2018).
13. Farahmandjou M. and Golabiyan N. Solution combustion

preparation of nano-Al_2O_3: synthesis and characterization. *Transp. Phenom. Nano. Micro. Scales.* **3**: 100-105 (2015).
14. Farahmandjou M. Synthesis of ITO Nanoparticles Prepared by Degradation of Sulfide Method. *Chin. Phys. Lett.* **29**: 077306-9 (2012).
15. Farahmandjou M. and Golabiyan N. Synthesis and characterization of Alumina (Al_2O_3) nanoparticles prepared by simple sol-gel method. *Int. J. Bio-Inorg. Hybr. Nanomater.* **5**: 73-77 (2016).
16. Jurablu S., Farahmandjou M. and Firoozabadi T.P. Multiple-layered structure of obelisk-shaped crystalline nano-ZnO prepared by sol–gel route. *J. Theoretical. Appl. Phys.* **9**: 261–266 (2015).
17. Dastpak M., Farahmandjou M. and Firoozabadi T.P. Synthesis and preparation of magnetic Fe-doped CeO_2 nanoparticles prepared by simple sol-gel method. *J. Supercond Nov. Magn.* **29**: 2925-2929 (2016).
18. Motaghi S.and Farahmandjou M. Structural and optoelectronic properties of Ce-Al_2O_3 nanoparticles prepared by sol-gel precursors. *Mater. Res. Express.* **6**: 045008 (2019).
19. Zarinkamar M., Farahmandjou M. and Firoozabadi T.P. One-step synthesis of ceria (CeO_2) nano-spheres by a simple wet chemical method. *J. Ceram. Proc. Res.* **17**: 166-169 (2016).
20. Farahmandjou M.and Soflaee F.Synthesis of Iron Oxide Nanoparticles using Borohydride Reduction. *Int. J. Bio-Inorg. Hybr. Nanomater*. **3**: 203-206 (2014).
21. Farahmandjou M. and Salehizadeh S.A. The optical band gap and the tailing states determination in glasses of TeO_2-V_2O_5-K_2O system. *Glass Phys. Chem.* **39**: 473-479 (2013).
22. A Khodadadi, M Farahmandjou, M Yaghoubi, AR Amani. Structural and optical study of Fe^{3+}-doped Al_2O_3 nanocrystals prepared by new sol gel precursors. *Int. J. Appl. Ceram. Technol.* **16**: 718-726 (2019).
23. Honarbakhsh S., Farahmandjou M. and Behroozinia S. Synthesis and characterization of iron cobalt (FeCo) nanorods prepared by simple Co-precipitation method. *J. Fund. Appl. Sci.* **8**: 892-900 (2016).
24. Behrouzinia S., Salehinia D., Khorasani K. and Farahmandjou M. The continuous control of output power of a CuBr laser by a pulsed external magnetic field. *Opt. Commun.* **436**: 143-145 (2019).
25. Farahmandjou M. and Motaghi S. Sol-gel Synthesis of Ce-doped α-Al_2O_3: Study of Crystal and Optoelectronic Properties. *Opt. Commun.* **441**: 1–7 (2019).
26. Jafari A., Khademi S., Farahmandjou M., Darudi A. and Rasuli R. Structural and optical properties of Ce^{3+}-doped TiO_2 nanocrystals prepared by sol-gel precursors. *J. Electron. Mater.* **47**: 6901–6908 (2018).
27. Khodadadi A., Farahmandjou M. and Yaghoubi M. Investigation on synthesis and characterization of Fe-doped Al_2O_3 nanocrystals by new sol–gel precursors. *Mater. Res. Express.* **6**: 025029 (2019).
28. Farahmandjou M. and Soflaee F. Polymer-Mediated Synthesis of Iron Oxide (Fe_2O_3) Nanorods. *Chin. J. Phys.* **53**: 080801-9 (2015).
29. Farahmandjou M. and Soflaee F. Synthesis and characterization of α-Fe_2O_3 nanoparticles by simple co-precipitation method. *Phys. Chem. Res.* **3**: 193-198 (2015).
30. Farahmandjou M. Magnetocrystalline properties of Iron-Platinum (L_{10}-FePt) nanoparticles through phase transition. *Iran. J. Phys. Res.* **16**: 1-5 (2016).
31. Shadrokh S., Farahmandjou M. and Firozabadi T.P. Fabrication and Characterization of Nanoporous Co Oxide (Co_3O_4) Prepared by Simple Sol-gel Synthesis. *Phys. Chem. Res.* **4**: 153-160 (2016).
32. Farahmandjou M., Honarbakhsh S. and Behrouzinia S. PVP-Assisted Synthesis of Cobalt Ferrite ($CoFe_2O_4$) Nanorods. *Phys. Chem. Res.* **4**: 655-662 (2016).
33. Farahmandjou M. Synthesis and Structural Study of L_{10}-FePt nanoparticles. *Turk. J. Engin. Environ. Sci.* **34**: 265-270 (2010).
34. Farahmandjou M., Honarbakhsh S. and Behrouzinia S. FeCo Nanorods Preparation Using New Chemical Synthesis. *J. Supercond. Nov. Magn.* **31**: 4147–4152 (2018).
35. Farahmandjou M. Effect of oleic acid and oleylamine surfactants on the size of FePt nanoparticles. *J. Supercond. Nov. Magn.* **25**: 2075-2079 (2012).
36. Sebt S.A., Parhizgar S.S., Farahmandjou M., Aberomand P. and Akhavan M. The role of ligands in the synthesis of FePt nanoparticles. *J. Supercond. Nov. Magn.* **22**: 849-854 (2009).
37. Steele B.C.H. Appraisal of $Ce_{1-y}Gd_yO_{2-y/2}$ electrolytes for IT-SOFC operation at 500°C. *Solid. State. Ion.* **129**: 95-110 (2000).
38. Bao H., Chen X., Fang J., Jiang Z. and Huang W. Structure-activity relation of Fe_2O_3–CeO_2 composite catalysts in CO oxidation. *Catal. Lett.* **125**: 160-167 (2008).
39. Tessier F. Chevré F. Munoz F., Merrdignac Conanec O., Marchand R., Bouchard. M. and Colbeau Justin C. Powder preparation and UV absorption properties of selected compositions in the CeO_2–Y_2O_3 system. *J. Solid State Chem.* **181**: 1204-1212 (2008).
40. Higashi K., Sonoda K., Ono H., Sameshima S. and Hirata Y. Characterization of Rare-Earth-Doped Ceria Powders Derived from Oxalate Coprecipitate. *Key Eng. Mater.* **25**: 159-160 (1999).
41. Zhang T., Hing P., Huang H. and Kilner J. Densification, microstructure and grain growth in the CeO_2–Fe_2O_3 system ($0 \leqslant Fe/Ce \leqslant 20\%$). *J. Eur. Ceram. Soc.* **21**: 2221-2228 (2001).
42. Zhang T.S., Ma J., Kong L.B., Zeng Z.Q., Hing P. and Kilner J.A. Final-stage sintering behavior of Fe-doped CeO_2. *Mater. Sci. Eng. B.* **103**: 177-183 (2003).
43. 43. Scherrer P. Bestimmung der Grosse und der Inneren Struktur von Kolloidteilchen Mittels Rontgenstrahlen. *Nachr. V. d. Gesellsch. d. Wissensch..Math. Phys. Kl. Gotting.* **2**: 98-100 (1918).